

2RE J0241 – 525: a nearby post-T Tauri visual binary system

R. D. Jeffries,¹ D. A. H. Buckley,² D. J. James³ and J. R. Stauffer⁴

¹Department of Physics, Keele University, Keele, Staffordshire ST5 5BG

²South African Astronomical Observatory, PO Box 9, Observatory 7935, Cape, South Africa

³School of Physics and Space Research, University of Birmingham, Edgbaston, Birmingham B15 2TT

⁴Smithsonian Astrophysical Observatory, 60 Garden Street, Cambridge, MA 02138, USA

Accepted 1996 March 8. Received 1996 March 4; in original form 1995 November 27

ABSTRACT

We present high-spatial-resolution X-ray observations, photometry and spectroscopy of the two low-mass, active stars proposed as optical counterparts to the extreme ultraviolet source 2RE J0241 – 525 (=EUVE J0241 – 530). It is confirmed that both stars, which are of types dK7e and dM3e and separated by 22 arcsec, are sources of soft X-ray emission and exhibit substantial chromospheric activity. Radial velocity measurements indicate that the two components are physically associated and most probably single. The projected equatorial velocities are measured as 75 ± 3 and 11.7 ± 0.7 km s⁻¹ for the hotter and cooler components respectively and, whilst the hotter component has a relatively high photospheric lithium abundance, $\log N(\text{Li}) = 1.5 \pm 0.2$, we are unable to detect any lithium in the cooler star. Isochrone fitting to this ‘mini-cluster’ yields an age of 3–70 Myr and a distance of 19–60 pc. An empirical comparison of the lithium abundances with those for similar stars in young clusters and associations suggests a narrower age range of 5–30 Myr and a corresponding distance of 26–50 pc. We conclude that this object is a nearby post-T Tauri system, but we cannot locate any possible birth site. It appears unlikely that the system can have been ejected from a nearby open cluster in a two- or three-body encounter.

Key words: stars: activity – stars: individual: 2RE J0241 – 525 – stars: late-type – stars: pre-main-sequence – stars: rotation – X-rays: stars.

1 INTRODUCTION

The *ROSAT* X-ray/extreme ultraviolet (EUV) satellite completed a successful all-sky survey in 1991. The initial results from the UK-built EUV Wide Field Camera (WFC) have been published in the form of a bright-source catalogue (Pounds et al. 1993) and in the more comprehensive ‘2RE’ catalogue (Pye et al. 1995), which contains 479 EUV sources. The majority of these sources are magnetically active late-type stars which emit EUV photons from a hot corona that is confined and heated by a magnetic field, which is in turn generated in the stellar convection zone by the interaction of differential rotation and cyclonic motions – a mechanism known as the dynamo process. Empirically, rapid rotation appears to be the key to these phenomena, and it has been shown that there are two main subclasses of EUV-bright, magnetically active stars, namely those that rotate rapidly because they are in tidally locked, short-

period binary systems (Jeffries, Bertram & Spurgeon 1995), and those that are single and rotate rapidly because they are young and have not yet lost a substantial amount of angular momentum (Jeffries 1995, hereafter J95).

Single, ultrafast rotating ($v \sin i > 40$ km s⁻¹), low-mass stars are rare amongst the field-star population, but are common in the young Pleiades and α Persei clusters (e.g. Stauffer, Hartmann & Jones 1989b; Stauffer 1991). The known examples of rapidly rotating field stars include AB Dor, HK Aqr, HD 197890, BD + 22° 4409 and 2RE 1816 + 541, and have spectral types of K0 to M2, periods from 0.3 to 0.8 d and projected equatorial velocities ($v \sin i$) up to 170 km s⁻¹ (see Young, Skumanich & Harlan 1984; Innis et al. 1988; Anders et al. 1993; Jeffries et al. 1994a; Jeffries, James & Bromage 1994b). These objects are much closer than stars of equivalent spectral type in the Pleiades, and are important because detailed observations can be performed to investigate the operation of the dynamo at

extreme rotation rates (e.g. Collier-Cameron & Unruh 1994; Robinson et al. 1994) and to explore how ultrafast rotating stars in young clusters lose vast amounts of angular momentum in their early lives (e.g. Collier-Cameron & Robinson 1989; Jeffries 1993).

Less extreme examples of young, rapid rotators have been found by virtue of their photospheric lithium abundances. Li is rapidly depleted in cool stellar atmospheres, because mixing processes bring material from interior regions that are hot enough to burn Li in p, α reactions. The equivalent width (EW) of the Li I line at 6708 Å has been used as an empirical age indicator by several authors (e.g. Tagliaferri et al. 1994; Favata et al. 1995; J95) to show that the low-mass content of X-ray and EUV surveys contain many stars at least as young as the Pleiades (age ~ 70 Myr). J95 has gone further than this, and shown that the ultrafast rotators and Li-rich low-mass stars may share a common evolutionary origin, because they have very similar space motions to the Pleiades, and also to a kinematic group of young, early-type stars in the solar vicinity, known as the Local Association.

Some of the Li-rich stars investigated by J95 are in visual binary systems, where, if the components are physically associated rather than being in the same line of sight, one can presumably be confident that the components have the same age and composition (see also Martín, Magazzù & Rebolo 1992, Pallavicini, Pasquini & Randich 1992 and Martín & Brandner 1995). These are of special interest because they form ‘mini-clusters’, where, in principle, the components could be matched to isochrones on colour-magnitude diagrams in order to obtain more reliable age and distance estimates. Furthermore, comparison could also be made between the Li abundances seen in both components and theoretical isochrones of Li depletion (e.g. d’Antona & Mazzitelli 1994).

Even younger late-type stars have been found in X-ray surveys of star formation regions and have been variously classified as either classical T Tauri stars (CTTS), weak-lined T Tauri stars (WTTS) or post-T Tauri stars (PTTS) (e.g. Walter et al. 1988; Neuhäuser et al. 1995a, and references therein). The distinction between CTTS and WTTS is usually made upon the strength of emission lines, veiling of the optical spectrum, and the strength of any infrared (IR) excess. In WTTS the $\text{H}\alpha$ emission is thought to be mainly chromospheric and is smaller than about 5 Å; there is little veiling of the optical spectrum, and little or no IR excess. In CTTS much greater $\text{H}\alpha$ emission is seen along with optical veiling and a prominent IR excess. It is generally assumed that these phenomena relate to the presence or not of active accretion and circumstellar gas or dust. In recent years, some evidence has emerged that there is an evolutionary link between WTTS and CTTS, in that WTTS are simply CTTS that have dispersed their discs, spun up and become more magnetically active (Bouvier et al. 1993a,b; Edwards et al. 1993; Neuhäuser et al. 1995a), although this is confused by the fact that CTTS and WTTS are found at the same age. PTTS were postulated by Herbig (1978) to be a slightly older generation of T Tauri stars that might be more widely dispersed from their birth sites. This view is supported by X-rays surveys of Orion (Sterzik et al. 1995), where a widely distributed WTTS population is found. It seems that the distinction between PTTS and WTTS may

only be their closeness to a region of star formation. Several of the rapidly rotating, Li-rich field stars, referred to above, have been labelled as PTTS in the past.

In this paper, we present new spectroscopic, photometric and high-spatial-resolution X-ray observations of a visual binary system that is the proposed optical counterpart to the EUV source 2RE J0241–525 (Mason et al. 1995). We show that the components are physically associated, and that both stars are extremely active and rapidly rotating. From isochrone fitting and a consideration of the observed Li abundances, it seems likely that neither component has evolved to the zero-age main sequence (ZAMS), and that the system is similar to WTTS, but is not associated with any particular star formation region.

2 OBSERVATIONS

2.1 ROSAT HRI observations

The WFC source 2RE J0241–525 was detected at the position $02^{\text{h}} 41^{\text{m}} 45.2^{\text{s}}$, $-52^{\circ} 59' 38''$ (J2000.0) with a positional error of 44 arcsec and count rates of 2.5×10^{-2} and 1.4×10^{-2} count s^{-1} in the S1 and S2 filters (see Pye et al. 1995 for details). In the WFC optical identification programme, Mason et al. (1995) have identified the EUV source with two dMe stars, inside the WFC error circle, separated by 22 arcsec (see Fig. 1). Ball & Bromage (1995) have reported that the northern dMe star exhibits considerable U -band flare activity. A corresponding source, EUVE J0241–530, was also seen in the subsequent *Extreme Ultraviolet Explorer* (EUVE) sky survey at a position nearly coincident with the WFC source. This also contains the two counterparts within its nominal 1-arcmin error circle (Bowyer et al. 1994). The spatial resolution of the WFC (or EUVE) is insufficient to resolve this pair, but new observations were obtained with the ROSAT High-Resolution Imager (HRI) on 1992 December 10–11.

The HRI has a field of view approximately 38×38 arcmin², is sensitive to photons in the 0.2–2.0 keV range and has a spatial resolution of about 3 arcsec on-axis (see Pfeffermann et al. 1986; David et al. 1992). The central part of the 3036-s HRI exposure is shown in Fig. 1 in contour form, superimposed on an optical image of the same field, obtained from the Space Telescope Science Institute digitized sky survey. Also marked is the WFC error circle. It is clear from Fig. 1 that the two candidate stars, which we will call north (N) and south (S), are both sources of soft X-ray emission, and therefore likely to contribute to the EUV emission seen by the WFC and EUVE.

The count rates and positions of the X-ray sources have been determined by a maximum-likelihood point-source searching (PSS) method (part of the Starlink ASTERIX package), which optimizes both source and background strengths with respect to the Cash likelihood statistic (Allan 1992). The background was very low indeed, at approximately 0.014 count s^{-1} arcmin⁻². Raw counts were corrected for the exposure time, dead-time, quantum efficiency variations and vignetting, assuming a mean photon energy of 1 keV, to give an on-axis count rate. These count rates were converted to an X-ray flux (0.1–2.4 keV), assuming a conversion factor of 1 count being equivalent to 4.4×10^{-11} erg cm^{-2} , which is appropriate for a 10^7 K optically thin plasma, and negligible interstellar absorption (David et al. 1992).

2RE J0241 – 525

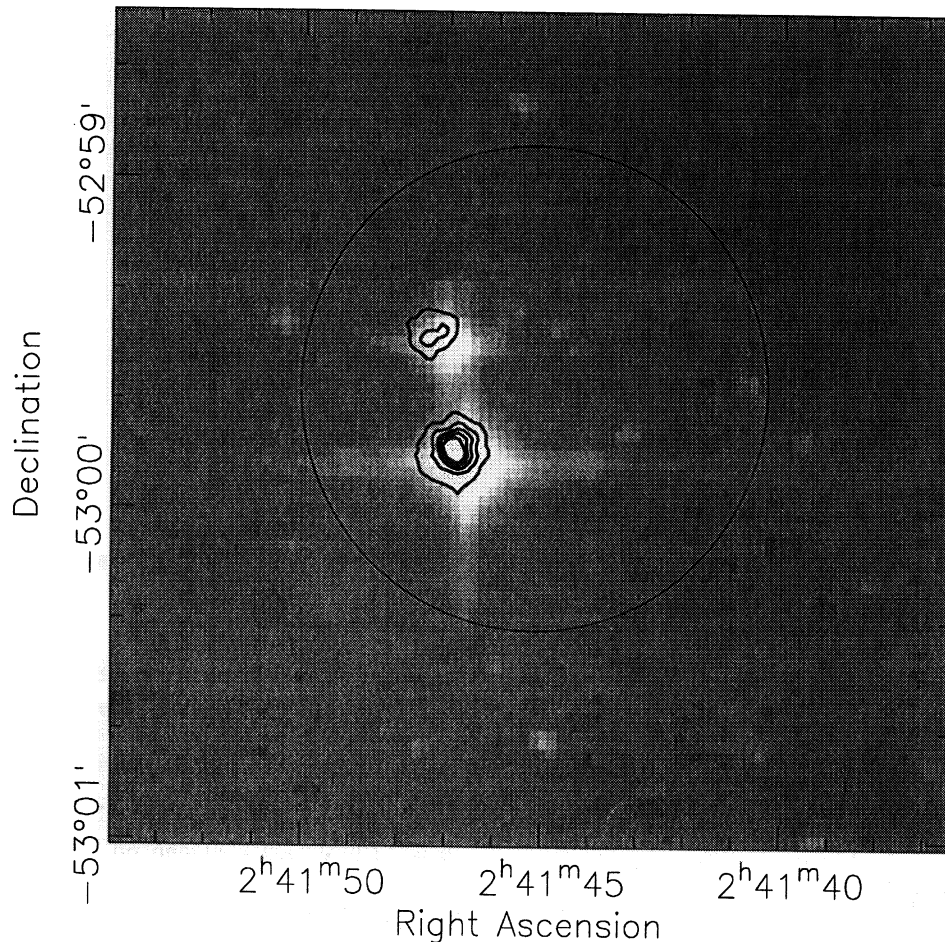


Figure 1. Contoured HRI image (0.2–2.0 keV) of the 2RE J0241 – 525 field superimposed on an optical image of the field. The circle represents the position of the WFC source error circle.

Table 1. PSS results.

	RA J2000.0	Dec	Error arcsec	Raw counts	Flux cts/ks	Flux (0.1–2.4 keV) ($\times 10^{-13}$ erg cm $^{-2}$ s $^{-1}$)
2RE J0241–525N	02 41 47.34	-52 59 28.0	0.5	186 \pm 19	59 \pm 6	13.0 \pm 1.3
2RE J0241–525S	02 41 46.84	-52 59 49.3	0.2	628 \pm 36	202 \pm 11	44.7 \pm 2.4

The PSS results and X-ray fluxes are given in Table 1. Comparison with coordinates in the Hubble guide star catalogue (version 1.1) gives position discrepancies for the north and south components (in the sense X-ray position minus optical position) of 1.9 and 2.4 arcsec in RA, and 2.1 and 2.3 arcsec in Dec. Given the uncertainties in the X-ray and optical positions, we conclude that these shifts are consistent, and that they are not unusually large for HRI observations.

The HRI observations were split into two observing slots, separated by 4.5 h. Time series were constructed for each component of 2RE J0241 – 525, using background from an

annulus surrounding both sources. The background-subtracted time series were then corrected for dead-time, vignetting and variable quantum efficiency, and are shown in Fig. 2, where the north component has been displayed in 200-s bins and the south component in 100-s bins. Clear variability is seen in the south component. The mean count rate in the first observing slot is 0.127 ± 0.018 count s $^{-1}$, whereas in the second slot the count rate is 0.275 ± 0.029 count s $^{-1}$. The corresponding means in the north component are 0.056 ± 0.006 and 0.061 ± 0.007 count s $^{-1}$, and there is no evidence for variability. The cause of the variability in the south component could be flaring or rotational

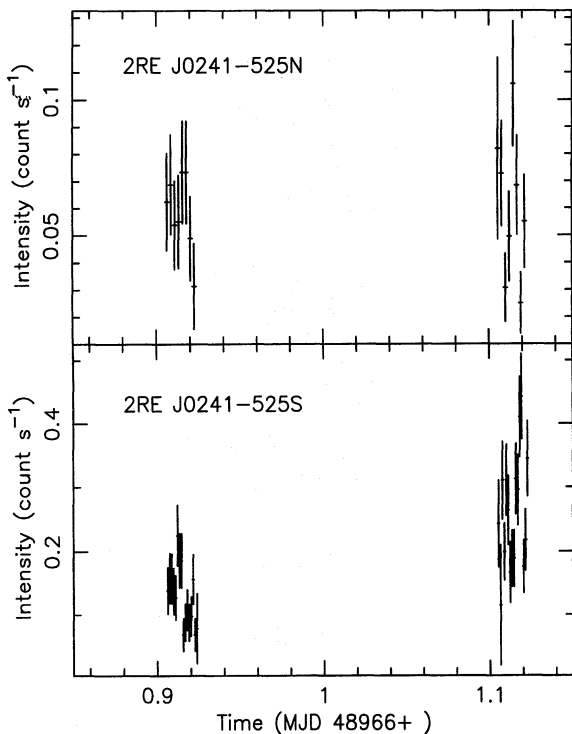


Figure 2. Time series of the HRI observations (0.2–2.0 keV) for the north and south components of 2RE J0241–525. The north component is in 200-s time bins, while the south component is in 100-s time bins.

modulation. The system would be an interesting target for a longer follow-up observation.

2.2 Photometry

UBV (Johnson system) (*RI*)_C (Cousins system) photoelectric photometry of the proposed optical counterparts was performed on the 0.75-m telescope of the South African Astronomical Observatory (SAAO) on 1992 December 17 with a single-channel photometer. A 13-arcsec aperture was used and the seeing was approximately 1 arcsec (FWHM), so contamination between the components should be negligible. Extinction values were determined from Cousins E-region standards (Menzies et al. 1989) and standard magnitudes derived from the well-determined colour equations at SAAO. *UBV(RI)*_C magnitudes are listed in Table 2.

2.3 Low- and intermediate-resolution spectroscopy

Low- and intermediate-resolution spectra of the optical counterparts were obtained in 1991 December with the 1.9-m telescope at SAAO, equipped with the Royal

Greenwich Observatory UNIT spectrograph and the Reticon Photon Counting System. Three separate wavelength ranges were covered: (i) 3400–6800 Å at a resolution of 6 Å, (ii) 3600–4200 Å at a resolution of 1.4 Å, and (iii) 5800–6800 Å at a resolution of 2.0 Å. Spectra were flat-fielded with long quartz lamp exposures and corrected for atmospheric extinction using data from Spencer-Jones (1980). Wavelength calibration was achieved by reference to argon arc lamp spectra. Absolute flux calibration was attempted with exposures of flux standards from Stone & Baldwin (1983). Because the slit-width was set at about 1.6 arcsec, the observations cannot be considered spectrophotometric. Nevertheless, Doyle et al. (1990) have shown, with the same instrumentation, that this approach can yield fluxes accurate to 20 per cent, although we conservatively estimate our errors to be within a factor of 2.

Fig. 3 shows the low-resolution spectra of the optical counterparts. Spectral types were estimated from the depression of the TiO bandheads at 4760, 5167 and 5548 Å and the MgH bandhead at 4780 Å, relative to the local continuum. These temperature-sensitive indices have been calibrated by Mathioudakis (1992). From these measurements, spectral types of dK7 and dM3 are estimated, with an uncertainty of \pm half a spectral subclass. Balmer emission lines are clearly evident in the spectrum of the cooler, north component, as well as Ca II H and K emission lines. There is also evidence for H α and Ca II H and K emission in the south component, but this is more obvious in the higher resolution spectra (see Fig. 4). Where there is sufficient signal, chromospheric emission line fluxes have been calculated by fitting Gaussian profiles above the local continuum level. These fluxes are given in Table 3.

Intermediate-resolution spectra in the blue and red wavelength ranges are shown in Fig. 4. Again, chromospheric emission lines are clearly visible, this time in both the north and south components. Fluxes are calculated by fitting Gaussians above the local continuum, and the results are given in Table 3. Also given are the EWs of the H α emission lines, which are of more utility in comparisons with other work. On 1991 December 26/27, 2RE J0241–525N was monitored at H α for approximately 3 h, between 23:00 UT and 02:00 UT, with 60-s exposures. No evidence for any significant variability was found, either on short-time-scales, or over the length of the monitoring period. The mean H α EW was 5.57 Å from 150 spectra, with a standard deviation of 0.85 Å, compatible with the estimated EW error for each spectrum.

2.4 High-resolution spectroscopy

High-resolution spectra of 2RE J0241–525 were obtained with echelle spectrographs at the Mount Stromlo (MSO)

Table 2. Photoelectric photometry.

	HJD 2448900+	V	B-V	U-B	V-R _C	V-I _C
2RE J0241-525N	74.345	12.167 \pm 0.003	1.484 \pm 0.006	0.984 \pm 0.014	1.055 \pm 0.004	2.372 \pm 0.003
2RE J0241-525S	74.352	10.276 \pm 0.004	1.258 \pm 0.003	0.930 \pm 0.007	0.808 \pm 0.002	1.595 \pm 0.002

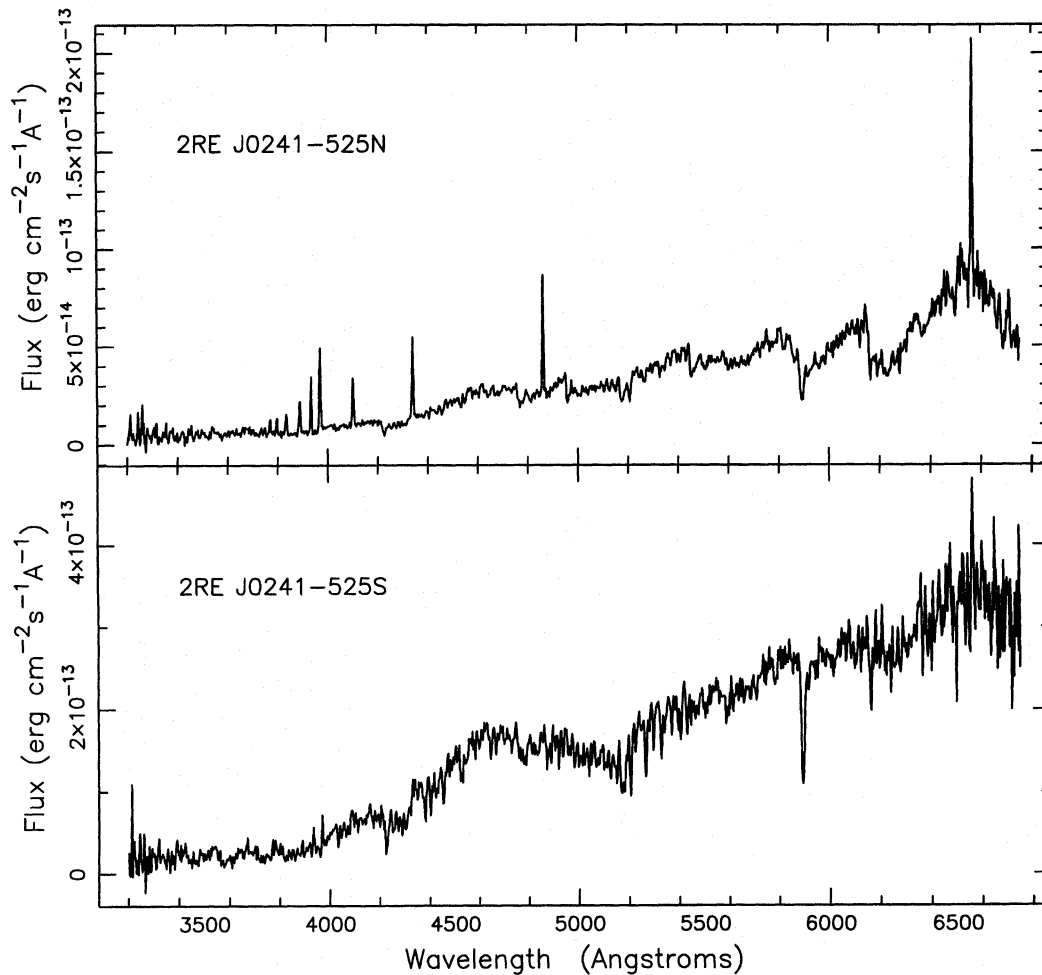


Figure 3. Low-resolution SAO spectra of the north and south components of 2RE J0241 – 525.

1.9-m telescope on 1994 June 22 (one spectrum of the south component), at the Cerro Tololo Inter-American Observatory (CTIO) 4-m telescope on 1995 January 15 (one spectrum each of the north and south components) and at the Anglo-Australian Observatory 3.9-m telescope (AAT) on 1995 January 21 (south component) and 22 (both components). The MSO observations were performed with a 79 line mm^{-1} grating, a square 2048 pixel Tektronix CCD and a 2-arcsec slit-width that yielded a resolution of 0.15 \AA at H α . The CTIO observations used a 31.6 line mm^{-1} grating, a square 2048 pixel Tektronix CCD and a 0.8-arcsec slit to give a 2-pixel resolution of about 0.15 \AA at H α . The AAT observations used a 79 line mm^{-1} grating, a square 1024 pixel Tektronix CCD and a 1.2-arcsec slit which gave a resolution of 0.16 \AA at H α . The CTIO spectra were debiased, flat-fielded and extracted (by JRS) using IRAF routines, while the MSO and AAT spectra were reduced using the ECHOMOP package (Mills & Webb 1994). In all cases, the slit-length was long enough to allow sky subtraction of the spectra without overlapping the adjacent orders. The signal-to-noise ratios of the AAT and CTIO spectra were in the range 60–90 per pixel, while the MSO spectrum was poorer, with a signal-to-noise ratio of 30.

The spectra were used to obtain heliocentric radial and rotational velocities using cross-correlation techniques (e.g.

Tonry & Davis 1979). The spectral ranges used were $\lambda\lambda 5875\text{--}5955$ for the MSO spectrum, $\lambda\lambda 6640\text{--}6750$ and $\lambda\lambda 7770\text{--}7870$ for the CTIO spectra, and $\lambda\lambda 5670\text{--}5732 \text{ \AA}$ for the AAT spectra. Radial velocity zero-points were set by reference to spectra of several radial velocity standard stars. For the CTIO spectra these were Gliese 205, 273 and 447, while for the AAT and MSO spectra HR 1829, 3748, 4182 and 5384 were used. Projected equatorial velocities ($v \sin i$) were obtained similarly, by calibrating the FWHM of the cross-correlation peaks obtained with slowly rotating, inactive standard star spectra of types similar to 2RE J0241 – 525N + S, that were convolved with a range of limb-darkened rotational broadening functions. The results of these analyses are given in Table 4. The weighted mean radial velocities for the north and south components are $+11.6 \pm 0.7$ and $+12.0 \pm 1.5 \text{ km s}^{-1}$, with no evidence for significant variability. The weighted mean $v \sin i$ values for the north and south components are 11.7 ± 0.7 and $75 \pm 3 \text{ km s}^{-1}$.

The high-resolution echelle spectroscopy also includes a spectral order containing the neutral Li resonance doublet at 6708 \AA . Fig. 5 shows the spectral region around this line for both components. The Li I line is prominent in 2RE J0241 – 525S, but is not clearly present in 2RE J0241 – 525N. The EW of the Li I lines has been estimated

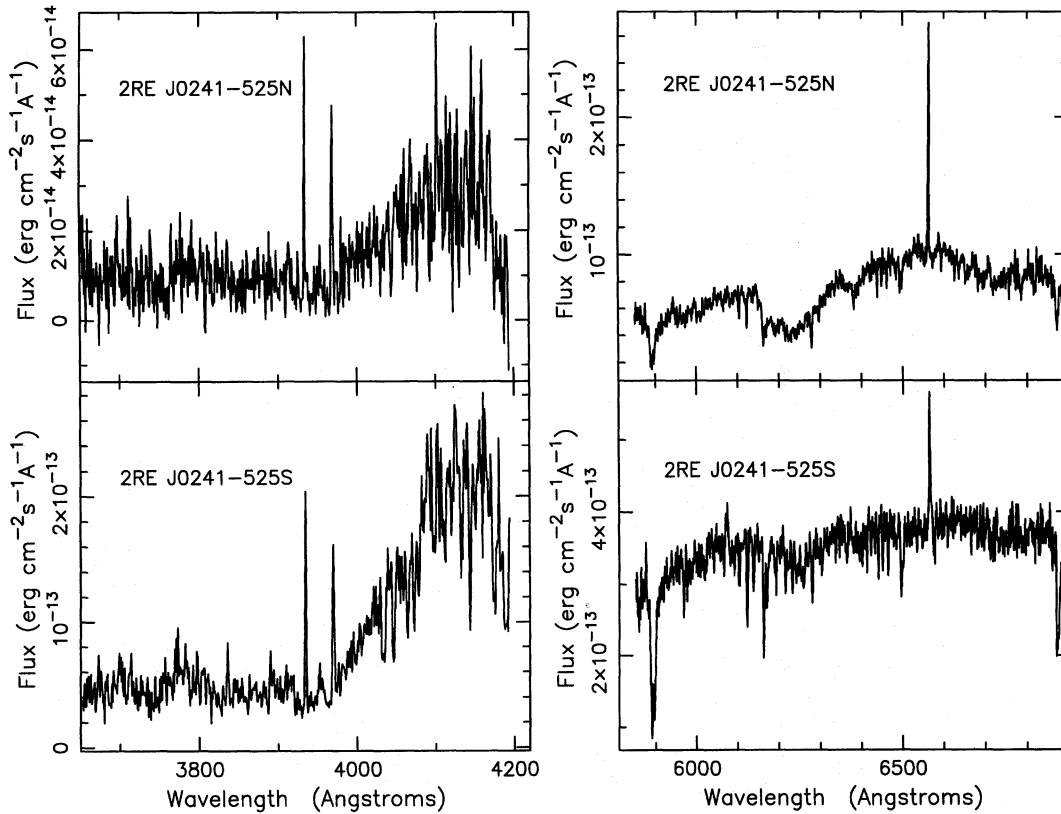


Figure 4. Intermediate-resolution SAAO spectra of the north and south components of 2RE J0241 – 525.

Table 3. Line fluxes in units of 10^{-13} erg cm $^{-2}$ s $^{-1}$, from the low- and intermediate-resolution spectroscopy.

Component	H α EW (Å)	H α	H β	H γ	H δ	Ca H+H ϵ	Ca K	H8	H9	H10	H11
2RE J0241-525N Low	5.8	5.2	2.8	2.0	1.3	2.4	1.2	0.92	0.53	0.31	0.27
2RE J0241-525S Low	0.7	2.4	-	-	-	1.2	0.80	-	-	-	-
2RE J0241-525N Int	5.7	5.8	-	-	0.80	1.2	1.1	-	-	-	-
2RE J0241-525S Int	1.1	4.1	-	-	-	1.5	1.6	-	-	-	-

by comparison with inactive, slowly rotating (and therefore presumably old and entirely depleted of Li) stars of similar spectral types. The standards used are Gliese 820B (type K7V) and Gliese 687 (type dM4). The standards are broadened to the same $v \sin i$ as the targets, and then shifted to the appropriate radial velocity and subtracted from the target spectra. The resultant residual at the Li I wavelength is then integrated to obtain the EW, which is given in Table 5. The advantage of this technique is that it minimizes the effects of blending with small surrounding lines, especially Fe I and molecular features, and allows an accurate estimate of the continuum level in the presence of rotational broadening. Of course, if the metallicities of standard and target are different, this might cause some systematic error, but the blended Fe I lines are small and this is a second-order effect. EWs measured from each spectrum are listed in Table 5. For 2RE J0241 – 525S the result of this analysis is that the weighted mean Li I 6708 Å EW is 293 ± 4 mÅ.

For 2RE J0241 – 525N, we are unable to identify any Li I 6708 Å line, even after the subtraction. It is conservatively estimated that the EW is less than 20 mÅ.

It was noted that the Li I 6708-Å EW measurements from MSO and CTIO for 2RE J0241 – 525S are lower than the other two (from the AAT) by 20–30 mÅ. This is a significant difference, because all the spectra have a similar resolution and have been analysed by subtracting the same standard star spectrum. The errors quoted in Table 5 are the random statistical errors in the integral of the residual Li I line in the subtracted spectra. Changes in the EW and profiles of the Li I 6708-Å feature have been seen before in rapidly rotating cool stars like V410 Tau and BD + 22° 4409 (Basri, Martín & Bertout 1991; Jeffries et al. 1994). These may be attributable to spots and plagues on the stellar surface causing small changes in the profile of the temperature-sensitive 6708-Å line. Fig. 6 shows the mean of the two AAT spectra, with the CTIO spectrum overlaid. The data have

been smoothed with a Gaussian of FWHM 20 km s^{-1} . The Li I profile seems considerably narrower in the CTIO spectrum (confirmed by Gaussian fitting), whereas the profiles of the Ca I 6718-Å feature seem comparable. This may not be surprising, because the Ca I line arises from an excited level and should be less temperature-sensitive.

The Li I EWs can be converted into abundances with published curves of growth. Using the Kirkpatrick et al. (1993) relationship between T_{eff} and $(V-I)_c$, T_{eff} is estimated to be 3600 and 3960 K for the north and south components. The NLTE curves of growth presented by Pavlenko et al. (1995) have been used to estimate the abundances on the conventional scale relative to $\log N(\text{H}) = 12$. The Li abundances of the hotter and cooler components are 1.5 and < -0.5 respectively. Alternatively, using the Bessell (1991) calibration of the $(V-I)_c$, T_{eff} relation, values of 4040 and 3500 K are obtained, leading to $\log N(\text{Li})$ values of 1.6 and < -0.5 . The differences between the NLTE treatment and an LTE approach are small at these temperatures, the dominant source of uncertainty will be error in the temperature scale used, and the errors in $\log N(\text{Li})$ are estimated to be ± 0.2 for the south component, but perhaps as much as ± 0.5 for the north component.

Chromospheric activity can also be gauged from the high-resolution spectra. The AAT, CTIO and MSO data contain the H α line, and the AAT data contain the Ca II 8542-Å feature, which is also a magnetic activity indicator (Soderblom et al. 1993b). The H α EWs were calculated relative to

a locally fitted continuum. Telluric lines were prominent in the AAT spectra, and were removed by comparison with a rapidly rotating B star. High-resolution H α spectra are shown in Fig. 7, and the measured EWs are listed in Table 5. The Ca II 8542-Å chromospheric emission has been measured in the same way as the Li I EWs. The low-activity standard stars were broadened, shifted and subtracted from the spectra of the two components, and the EW of the residual line at 8542 Å taken as the chromospheric contribution. These EWs are also given in Table 5, and the spectra are plotted in Fig. 8. The Ca II 8542-Å EWs were

Table 4. Radial and rotational velocities.

Star	HJD 2449500+	Radial Velocity km s^{-1}	$v \sin i$ km s^{-1}
2RE J0241-525N			
CTIO	233.53	$+11.6 \pm 2.0$	12.3 ± 1.0
AAT	239.94	$+11.6 \pm 0.7$	11.1 ± 1.0
2RE J0241-525S			
MSO	26.33	$+9.9 \pm 4.0$	71 ± 7
CTIO	233.53	$+11.0 \pm 3.0$	68 ± 7
AAT	238.95	$+13.3 \pm 3.1$	80 ± 5
AAT	239.93	$+12.5 \pm 2.4$	75 ± 5

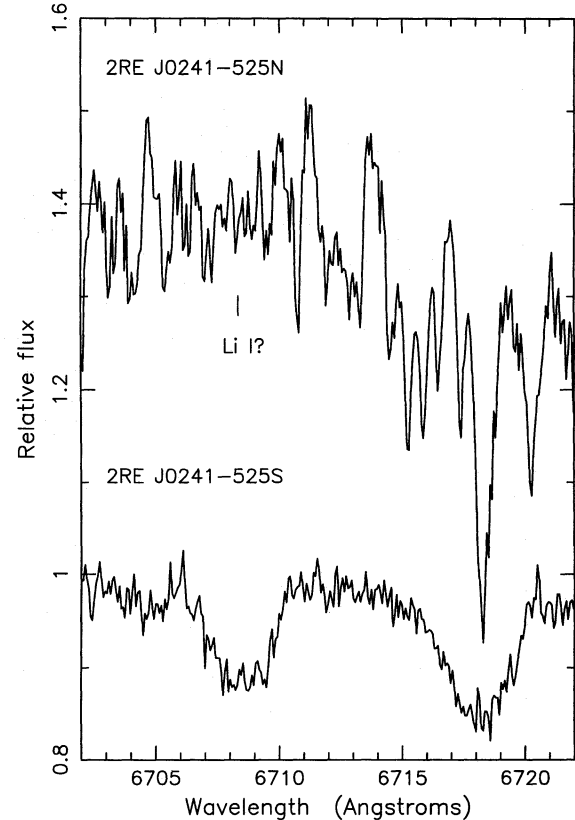


Figure 5. Normalized AAT echelle spectra in the vicinity of the Li I 6708-Å feature. The location of any possible Li I line is marked in the north component.

Table 5. High-resolution line EWs and fluxes.

Star	HJD 2449500+	Li I 6708Å EW (mÅ)	H α EW (Å)	Ca II 8542Å EW (Å)	$f_{\text{Ca II}}$ ($\times 10^{-13} \text{ erg cm}^{-2} \text{ s}^{-1}$)
2RE J0241-525N					
CTIO	233.53	< 25	3.30 ± 0.02	-	-
AAT	239.94	< 20	2.35 ± 0.02	0.63 ± 0.01	1.06 ± 0.02
2RE J0241-525S					
MSO	26.33	271 ± 15	0.81 ± 0.05	-	-
CTIO	233.53	277 ± 7	1.30 ± 0.04	-	-
AAT	238.95	308 ± 7	1.30 ± 0.04	1.07 ± 0.03	4.06 ± 0.11
AAT	239.93	298 ± 7	1.27 ± 0.04	1.07 ± 0.03	4.06 ± 0.11

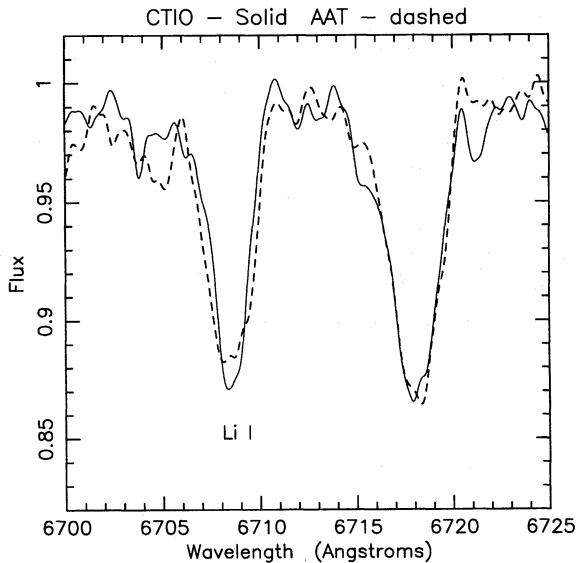


Figure 6. Normalized echelle spectra in the vicinity of the Li I 6708-Å feature. CTIO data (solid line) and AAT data (dashed line), illustrating possible profile variability. The spectra have been smoothed with a 20 km s⁻¹ FWHM Gaussian filter.

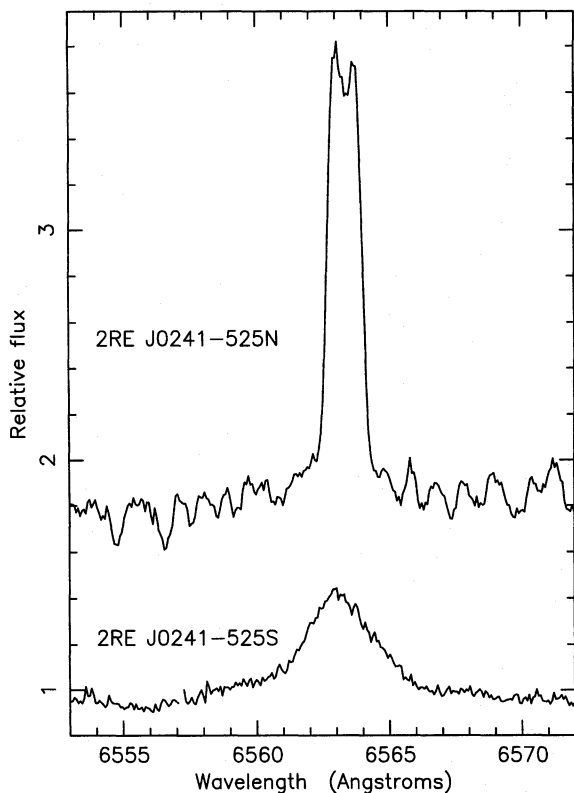


Figure 7. Normalized AAT echelle spectra in the vicinity of the H α feature.

converted into fluxes (for comparison purposes – see Section 3.3). This was achieved by assuming Johnson ($V-I$) colours of 1.93 and 2.94, using the calibration against spectral type in Johnson (1966), and then using the I_c magnitude to estimate the continuum flux at 8542 Å, assuming an absolute flux of 8.32×10^{-10} erg cm⁻² s⁻¹ Å⁻¹ for $I_c=0$. I_c

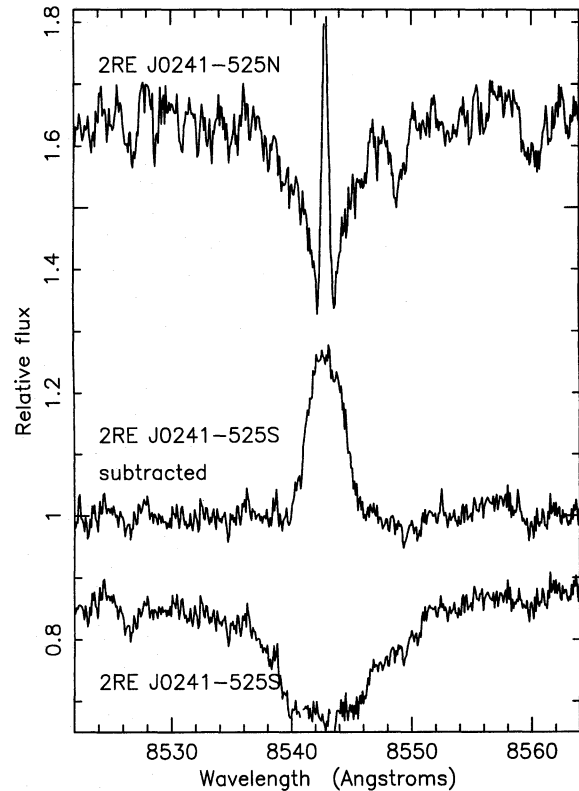


Figure 8. Normalized AAT echelle spectra in the vicinity of the Ca II 8542-Å feature. The central plot shows the spectrum of the south component (bottom) after subtraction of a low-activity standard star (HD 4628), and illustrates the chromospheric activity present.

actually has an effective wavelength of 9000 Å, but this will not greatly influence the results for these cool stars. The derived fluxes at the Earth are given in Table 5.

3 THE PHYSICAL AND EVOLUTIONARY STATUS OF 2RE J0241 – 525

3.1 The age of 2RE J0241 – 525 from isochrone fitting

From the similarity of the measured radial velocities in Table 4, it would seem that the north and south components of 2RE J0241 – 525 are part of a wide binary system. Fast rotating ($v \sin i > 10$ km s⁻¹) low-mass stars are relatively rare among field stars and are usually only found in open clusters (Stauffer & Hartmann 1986), and so the chances of finding two within the same WFC error circle, unless they were physically associated, seems too remote to be worth further consideration.

Low-mass stars are generally found to be rapidly rotating for one of two reasons: (i) they are in tidally locked, close binary systems, or (ii) they are young, and have not yet lost their birth angular momenta. In this case, the second explanation is more likely. The radial velocity measurements show no variability within quite tight limits compared with the $v \sin i$ values. However, the small number of measurements preclude a conclusive statement at this time. Nevertheless, one would generally expect radial velocity variations comparable to or larger than the $v \sin i$ value in

tidally locked binary systems, and it would therefore be quite improbable to obtain such consistent values (see Jeffries et al. 1994b for a detailed analysis of this argument), especially for 2RE J0241 – 525S.

Given then that the system is likely to be quite young, and that the two components are physically associated and therefore must be of similar age, it is possible to fit isochrones to try and determine the age and distance of the ‘mini-cluster’. For low-mass stars the most profitable colour–magnitude diagram to use is V versus $(V-I)_C$. The pitfalls in this process have been reviewed by Stauffer, Hartmann & Barrado y Navascues (1995). They found that the critical factor was the relationship adopted between effective temperature and $(V-I)_C$. Following the conclusions reached in that paper, we adopt the temperature scale of Bessell (1979) for $T_{\text{eff}} > 4500$ K and that of Kirkpatrick et al. (1993) for cooler atmospheres, and transform the evolutionary models of d’Antona & Mazzitelli (1994) on to the observational plane. The particular models used are those which use the Canuto & Mazzitelli (1990) convection theory and the opacities of Alexander, Augason & Johnson (1989). The bolometric corrections of Schmidt-Kaler (1982) are used for temperatures greater than 4000 K, and the bolometric corrections of Bessell (1991) for temperatures less than this. Stauffer et al. (1995) find that this procedure matches the empirical Pleiades isochrone over a wide range of $(V-I)_C$ at about 70 Myr, and conclude that age estimates based upon these assumptions are robust for a number of other evolutionary models, in the sense that similar isochrones are produced if a temperature scale is used that matches the empirical Pleiades isochrone at 70 Myr.

In Fig. 9 we show the results of our attempts to place both components of 2RE J0241 – 525 on to theoretical isochrones by varying the distance modulus. For isochrones at 3, 10, 35 and 70 Myr and the ZAMS, the distance modulus is adjusted to place 2RE J0241 – 525S on the isochrone. The corresponding distances are 52, 39, 28, 22 and 21 pc. In each case we can then see where 2RE J0241 – 525N lies relative to the same isochrone. To gain insight from this plot, one needs to consider the possible errors involved. Rapidly rotating, cool stars usually exhibit brightness variations associated with the rotation of cool, spotted regions around their surfaces. From similar objects (e.g. Jeffries et al. 1994a) we can estimate an error in the V magnitude of ± 0.1 and possibly ± 0.02 in $(V-I)_C$, although these would tend to be correlated in the sense that if $(V-I)_C$ increases due to coverage in cool spots, V would increase as well, and so the star would move approximately along the isochrone. Repeated measurements would assist in reducing this error. A more serious problem is systematic errors in the stellar evolution models. Comparisons with other evolutionary tracks produced by D. Vandenberg, F. Swenson (presented in Stauffer et al. 1995), and alternative opacity and convection models in d’Antona & Mazzitelli (1994), show that there can be about a 0.25-mag difference in the absolute magnitude of the 10-Myr isochrone, depending upon which model is used. This obviously has a corresponding effect on the distance modulus derived for 2RE J0241 – 525. Not only that, but there are small differences in the ‘gradient’ of the isochrones, amounting to about 0.1 mag over a range in $(V-I)_C$ covering the two components of 2RE J0241 – 525. The net effects of these errors are allowed for by assuming

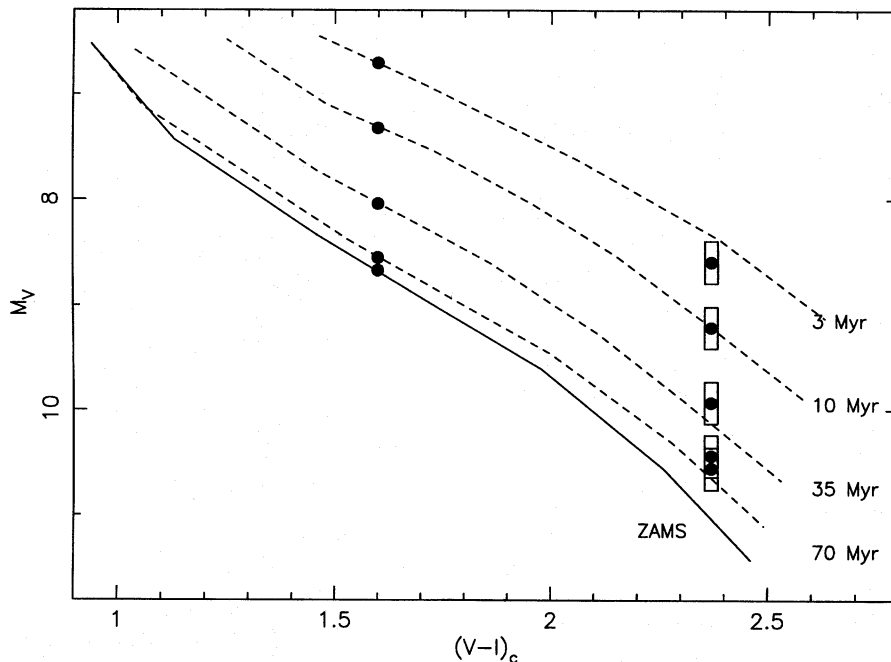


Figure 9. Isochrones in the observational V versus $(V-I)_C$ plane. Points corresponding to 2RE J0241 – 525N and S are superimposed, using distances (from top to bottom) of 52, 39, 28, 22 and 21 pc. Evolutionary models are from d’Antona & Mazzitelli (1994); conversion to the observational plane is via the $T_{\text{eff}}, (V-I)_C$ relationships proposed by Bessell (1979) and Kirkpatrick et al. (1993). The boxes around the cooler component represent possible error bounds due to systematic errors in the stellar evolution codes and brightness variations due to starspot modulation.

that the distance modulus is uncertain by about 0.3 mag, and that for the purposes of deriving an age, the cooler component can be assumed to have a net error bar of ± 0.2 in V and ± 0.03 in $(V-I)_C$, which allows for starspot modulation in both components and the uncertain isochrone slope.

From Fig. 9, we can conclude that the most favoured age for the 2RE J0241–525 system is between 3 and 70 Myr. The ZAMS isochrone is excluded by our analysis. When 2RE J0241–525S is placed upon the ZAMS isochrone, 2RE J0241–525N is 0.5 mag above it. Similarly, ages less than 3 Myr seem unlikely because 2RE J0241–525N would then be too faint relative to 2RE J0241–525S. It would be premature to rule out any age between about 3 and 70 Myr on the basis of the photometry alone. The corresponding distances (allowing for a further ± 0.3 error in the distance modulus) are from 60 to 19 pc.

3.2 The lithium abundance of the two components

The age of 2RE J0241–525 can be constrained by the measurements of Li abundance in two ways. First, by empirical comparison of the Li I EW with measurements from groups of stars of known age, it can be roughly deduced whether the system is younger or older. This is confused by any scatter present in Li I EW at a given age. Also, the absolute age is still dependent on particular evolutionary models chosen to describe cluster isochrones. Secondly, the absolute Li abundances can be compared with theoretical models of how the photospheric depletion proceeds with time, for stars of a given mass.

The reader should note that Fekel (1996) and Soderblom et al. (1996) have urged caution in using the Li abundance–age relationship, warning of instances where it can break down, especially in some cases where post-main-sequence objects, metal-poor Population II stars or close binary systems have been found to have high Li abundance. In this case, though, where both stars are very cool, appear to be single, and there is supporting evidence from the isochrones and rotation rates (see later) for a pre-main-sequence origin, we feel reasonably secure in performing age estimates based upon Li abundance. Perhaps of more concern are the hints in theoretical calculations by Swenson, Stringfellow & Faulkner (1990) that even small changes in metallicity can have a profound effect upon the rate of lithium depletion by altering conditions at the base of the convection zone. Their calculations do not extend to stars as cool as those considered here. Nevertheless, we have checked the metallicity of 2RE J0241–525S by synthesizing the spectral region between 5670 and 5732 Å in the AAT spectra, which contains many metal lines. We use Kurucz model atmospheres (Kurucz 1991), the Kurucz & Bell (1995) line list and the UCLSYN synthesis software (Smith 1992) to generate spectra at a range of metallicities. The temperature used was 4000 K, log gravity was 4.5, and $v \sin i$ was 75 km s⁻¹. We also perturbed all these parameters within their likely error bounds to investigate the effect of their uncertainties on the metallicity determination. From this analysis we find a best-fitting metallicity of -0.10 ± 0.15 .

The data for an empirical comparison come mainly from measurements of Li depletion among the low-mass stars in

the Pleiades (age 70 Myr – Soderblom et al. 1993a; García-López, Rebolo & Martín 1994), α Persei cluster (age 50 Myr; Balachandran, Lambert & Stauffer 1988), IC 2391/2602 (age 35 Myr; Stauffer et al. 1989a; S. Randich, private communication) and T Tauri stars in the Taurus–Auriga complex (age <1–20 Myr; Magazzù, Rebolo & Pavlenko 1992; Martín et al. 1994). The metallicities of these clusters are in the range -0.20 to $+0.11$ (Lyngå 1987) and therefore comparison with 2RE J0241–525S seems reasonable, although until further theoretical or observational work is done on the effects of small metallicity differences on Li depletion in cool stars, we should still be cautious about interpreting the results.

The first conclusion that can be arrived at from these comparisons, is that 2RE J0241–525S has a considerably higher Li I 6708 Å EW than stars of a similar colour in either the Pleiades, α Persei cluster, IC 2391 or 2602. Dr S. Randich (private communication) has new measurements of stars in IC 2391/2602 and finds that, for about a dozen stars with $(V-I)_C$ values between 1.3 and 1.9, the Li I 6708 Å EW varies from <50 mÅ to about 150 mÅ. From this it seems likely that 2RE J0241–525 is younger than IC 2391/2602. No Li I 6708-Å line has been detected in stars as cool as 2RE J0241–525N in the Pleiades, α Per or IC 2391/2602 clusters. Therefore our non-detection of the line does not give an upper limit to the age in this case. Li 6708-Å lines with EWs of several hundred mÅ have been found in WTTS and CTTS, with temperatures of ~ 3500 K and ages of <2 Myr, along with others at an age of 2 Myr with no detectable Li (Martín et al. 1994). The available evidence seems to suggest that Li depletion is not significant prior to this for very cool stars, presumably because their cores are not hot enough to burn Li. Martín et al. also present some data for WTTS at around 4000 K, similar to 2RE J0241–525S. These seem to show that these may remain undepleted of Li for somewhat longer, perhaps 3–5 Myr. This can be understood, because although in more massive stars, Li-burning central temperatures are reached more swiftly, a radiative core also develops which inhibits mixing of the depleted material. 2RE J0241–525S has clearly suffered some depletion. Its Li abundance is $\log N(\text{Li}) = 1.5 \pm 0.2$ compared with the generally accepted cosmic abundance of 3.2 ± 0.2 . Taken together, the empirical conclusion that can be reached, is that 2RE J0241–525 is younger than 35 Myr, but at least 5 Myr old, in agreement with the conclusions from the isochrone fitting.

The Li abundances can also be compared with theoretical models of depletion. Fig. 10 shows the abundances of 2RE J0241–525 compared with two sets of Li depletion isochrones from the models of d’Antona & Mazzitelli (1994). These are the set 1 and set 3 models from that paper, which use a solar metallicity and opacities from Alexander et al. (1989) together with the Canuto & Mazzitelli (1990) convection model (solid lines) or the standard mixing-length convection model (dashed lines). These two are presented to give an idea of the systematic differences between various models.

From Fig. 10, it does not seem that 2RE J0241–525 can be fitted by any single isochrone. Either the cooler component has suffered too much depletion, or the hotter component not enough. Martín et al. (1994) noted a similar trend in their observations of WTTS. They concluded that this

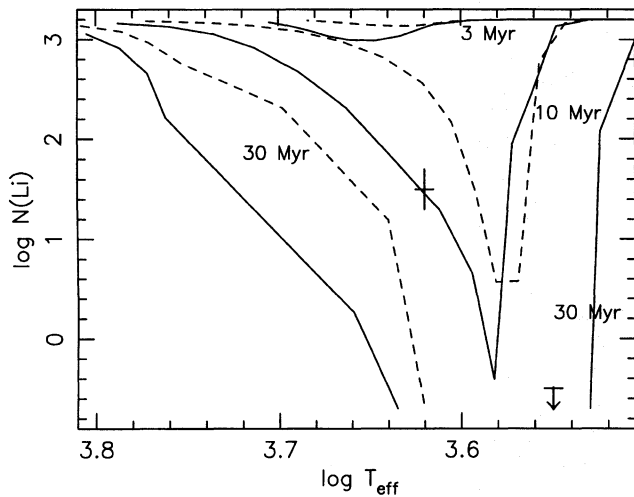


Figure 10. Isochrones of $\log N(\text{Li})$ versus effective temperature from the models of d’Antona & Mazzitelli (1994), normalized to a cosmic abundance of $\log N(\text{Li}) = 3.2$. Isochrones at 3, 10 and 30 Myr are plotted using their set 1 and set 3 models which both use Alexander et al. (1989) opacities together with the Canuto & Mazzitelli (1990) convection model (solid lines) or standard mixing-length theory (dashed lines). Points corresponding to 2RE J0241 – 525N and S are marked.

could best be explained if the cores of low-mass stars reached Li-burning temperatures more quickly than currently predicted by models. This would result in the sharp dip in $\log N(\text{Li})$ for $\log T_{\text{eff}} > 3.55$, moving to the right in Fig. 10, perhaps allowing the 10-Myr isochrones to fit both the hot and cool components of 2RE J0241 – 525. An alternative interpretation would be that 2RE J0241 – 525S is underdepleted with respect to 2RE J0241 – 525N, and that perhaps the system is as old as 30 Myr. This idea finds support from the observation that among the Pleiades and WTTS it seems that rapid rotation can inhibit depletion of Li relative to the predictions of standard stellar evolution models (Soderblom et al. 1993a; García-López et al. 1994; Martín et al. 1994). There is in any case a scatter in the Li abundances among K-type Pleiades of a given mass, which cannot be attributed to an age spread. Taken together, these properties preclude a more detailed comparison with theoretical isochrones, although the empirical comparisons should still be valid as long as we can assume that observations of one cluster or association are representative for stars at that age.

3.3 Rotation and magnetic activity

A further opportunity to empirically place 2RE J0241 – 525 in an evolutionary sequence is offered by the measurements of rotation and magnetic activity, because both show a general decline with age. The rotation rate of 2RE J0241 – 525S is higher than anything of a similar colour in the Hyades (age 600 Myr) but is comparable with some late K-type stars in the Pleiades and α Persei clusters (Stauffer 1991) and some WTTS with ages of a few Myr (Magazzù et al. 1992). The rotation rate of 2RE J0241 – 525N offers even less constraint, although most Hyads of a similar colour have $v \sin i < 10 \text{ km s}^{-1}$.

Similarly, only weak constraints can be placed on the age from the observed coronal and chromospheric activity. This is to be expected, as it is now believed that activity depends upon age implicitly because of the more fundamental rotation–activity and rotation–age relationships. The $H\alpha$ EW is variable (see Tables 3 and 5), but at its highest is larger than the upper envelope of the Hyades distribution with colour for both components (Stauffer et al. 1991, 1994a, b). However, the EWs of both components are compatible with stars of equivalent colour in both the Pleiades and IC 2391/2602 (Prosser, Stauffer & Kraft 1991; Stauffer et al. 1995).

Magnetic activity is often expressed as a ratio of the flux in a particular waveband or spectral line, to the bolometric flux. Bolometric corrections are taken from the calibration against $(V - I)_C$ of Bessell (1991), and bolometric fluxes of 1.94×10^{-9} and $4.77 \times 10^{-9} \text{ erg cm}^{-2} \text{ s}^{-1}$ are calculated for the north and south components of 2RE J0241 – 525 respectively. From these, we calculate the activity indices $\log L_x/L_{\text{bol}}$ from the 0.1–2.4 keV X-ray fluxes in Table 1, and $\log L_{\text{Ca II 8542}}/L_{\text{bol}}$ from the fluxes in Table 5.

We find $\log L_x/L_{\text{bol}}$ values of -3.17 and -3.03 for the north and south components respectively. Comparison with stars in the Hyades (Pye et al. 1994), Pleiades (Stauffer et al. 1994b) and IC 2602 (Randich et al. 1995) shows that there are stars at these colours and activity levels in all of these clusters, but that they are the most active stars in each cluster. This can be understood in terms of the rotation–activity paradigm, because although there are more rapidly rotating stars in both the Pleiades and IC 2602 compared with the Hyades, it seems that coronal activity saturates for $v \sin i > 15 \text{ km s}^{-1}$, at a value of $\log L_x/L_{\text{bol}} \sim -3$. Thus the X-ray activity of 2RE J0241 – 525 is simply consistent with the rotation rates we have measured and gives no further insight as to the evolutionary status of the system. This may not be the case for $\log L_{\text{Ca II 8542}}/L_{\text{bol}}$, which appears to increase, with little evidence for any saturation, as the rotation rate increases in low-mass stars (Soderblom et al. 1993b). Unfortunately, data have been published only for the Pleiades. Our values for this activity index, of -4.26 and -4.07 for the north and south components, lie near the upper envelope of the Pleiades observations, but seem consistent with the correlation with Rossby number (the ratio of rotation period to convective turnover time) presented by Soderblom et al. (1993b), so offer no further age constraint beyond that supplied by the rotation rates.

It is interesting to predict the true rotation period of the two component stars, which will, of course, depend on their inclination angles and radii. Using the isochrones shown in Fig. 9, we can estimate the distance, d , in pc at a given age. To calculate the radius we use a Barnes–Evans relationship, which assumes a linear proportionality between the surface brightness in V and the $(V - R)_C$ colour (see Barnes, Evans & Moffett 1978; Mathioudakis 1992):

$$\log \frac{R}{R_{\odot}} = -0.191 - 0.2V + 0.9(V - R)_C + \log d.$$

Then, because $Pv \sin i = 2\pi R \sin i$, where P is the rotation period, we can calculate $P/\sin i$ for both components, and these are given in Table 6 for a range of ages from 3 to 70 Myr. Theoretically, one might expect aligned rotation axes if the binary condensed from a cloud with uniform rotation,

Table 6. Predicted rotation periods.

Age (Myr)	Distance (pc)	R_N (R_\odot)	R_S (R_\odot)	$\left(\frac{P}{\sin i}\right)_N$ (hrs)	$\left(\frac{P}{\sin i}\right)_S$ (hrs)
3	52	1.10	1.57	114.2	25.4
10	39	0.82	1.18	85.1	19.1
35	28	0.59	0.85	61.2	13.7
70	22	0.47	0.66	48.8	10.7

but probably random alignments in cases where the stars form from fragmented clouds and then pair up some time later. Observationally, Hale (1994) has found random rotation axis orientation for binary separations greater than a few tens of au. The separation of the 2RE J0241–525 components is substantially larger than this (see Section 3.4), so we cannot assume alignment of the rotation axes.

From Table 6, it is apparent that, even in the absence of a parallax measurement, it may be possible to make further refinements in the age and distance estimates for 2RE J0241–525 by obtaining rotation periods for the two components. It is almost certainly feasible to do this by monitoring photometric modulation due to cool starspots on the stellar surface. Columns 5 and 6 of Table 6 are the *maximum* periods that the components can have at that particular age. Thus, for example, measuring a period of say 20 h for 2RE J0241–525S would indicate that the system is younger than 10 Myr, and is at a distance of at least 39 pc. On the other hand, measuring a period of 10 h would allow any of the ages considered here, with a decreasing inclination angle for decreasing age. It should be noted that, due to our discussion of uncertainty in the theoretical isochrones (see Section 3.1) of about ± 0.3 mag, it would be prudent to assume errors of about ± 15 per cent in the predicted radii and $P/\sin i$ values.

3.4 The origin of 2RE J0241–525

There are a few other wide binary systems like 2RE J0241–525 in which the hotter star is Li-rich and is accompanied by a low-mass dMe star. Examples include AB Dor, HD 155555, HD 21845 and BD + 17° 4799 (J95; Martín & Brandner 1995). There are also examples of Li-rich, late-type stars in visual binary systems with very young early-type stars (Martín et al. 1992; Pallavicini et al. 1992). 2RE J0241–525 appears to share a common evolutionary status with these systems. If 2RE J0241–525 is aged between 5 and 30 Myr, as suggested by the empirical evidence of the Li I 6708-Å EWs, then other indicators of youth might be present, such as an associated star formation region or T Tauri-like behaviour.

2RE J0241–525 appears to have no spatial association with any star formation region. The chromospheric emission lines are as strong as might be expected on the basis of their interpretation as magnetic-activity-related phenomena, but the H α emission would be weak for a CTTS. There is no veiling apparent in any of our spectra, compared with stars of similar spectral type, and there is no coincident source in the *Infrared Astronomical Satellite* (IRAS) point-

source catalogue that would suggest the presence of dust or a disc around either star. On the basis of this evidence we would not classify either component of 2RE J0241–525 as a CTTS. The Li abundances, rotation and magnetic activity of 2RE J0241–525S seem similar to many of the WTTS found in the Taurus–Auriga and Orion molecular cloud complexes (Walter et al. 1988; Bertout 1989). In addition, the $v \sin i$ value would be exceptionally high for a CTTS, but is reasonably common among WTTS (Bouvier et al. 1993a). This fits in with the currently favoured paradigm (see, e.g., Bouvier et al. 1993b), that the rotation rates of CTTS are regulated by magnetic coupling between the star and a disc. When the disc is dissipated the star can spin up, and so young stars without discs (WTTS) tend to rotate faster.

Sterzik et al. (1995) and Neuhäuser et al. (1995b) have found evidence for ‘haloes’ of WTTS around both the Orion and Taurus–Auriga star formation regions. They suggest that either these WTTS are older than most stars in the region (> 10 Myr), have unusually large velocity dispersions or, in some cases, may have been ejected from the star formation region in a three-body encounter. It is tempting to speculate that 2RE J0241–525 and perhaps many of the Li-rich, rapidly rotating field stars are simply more extreme examples of these runaway WTTS, in the sense that they are somewhat older and/or have slightly larger peculiar velocities with respect to their progenitor molecular clouds. J95 has suggested that many, if not the large majority, of young, Li-rich stars in the solar vicinity are part of a kinematic group known as the Local Association. The group is apparent in the space-motions of young early-type stars and also includes the Pleiades and α Persei clusters (Eggen 1983a,b). The hypothesis is that these stars were either ejected from young clusters, or more probably that the Local Association is the kinematic remnant of one or perhaps several star formation regions that emerged from molecular clouds in a gravitationally unbound state (Battistelli & Capuzzo-Dolcetta 1991; Lada & Lada 1991), and have a kinematic dispersion similar to that of molecular clouds in the solar vicinity.

Although we do not have proper motion information for 2RE J0241–525, the hypothesis that it is a member of the Local Association can be tested with its radial velocity. Using the group convergent point and speed ($\alpha = 89^\circ.7$, $\delta = -35^\circ.2$, $V_a = 26.5$ km s $^{-1}$; Eggen 1992), we can predict that a Local Association member at the position of 2RE J0241–525 should have a radial velocity of $+20.7$ km s $^{-1}$, compared with weighted means for the north and south components, $+11.6 \pm 0.7$ and $+12.0 \pm 1.5$ km s $^{-1}$. This discrepancy is not sufficient evidence to rule out Local Association membership if the one-dimensional radial velocity dispersion of the group is as large as the 6 km s $^{-1}$ suggested by J95, but neither does it particularly suggest Local Association membership. Perhaps this is not surprising as it is probable that 2RE J0241–525 is younger than the Pleiades or the α Persei clusters. Three younger kinematic associations that have been investigated in the past are the IC 2391 *supercluster*, which contains IC 2391 and many other young B stars in the solar vicinity, the Sco–Cen association and the Cas–Tau association. For the IC 2391 supercluster, which we presume has an age similar to that of the IC 2391 cluster itself, of about 35 Myr, Eggen (1991) gives a convergent point of $\alpha = 87^\circ.3$, $\delta = -12^\circ.4$, and a total

group speed of 27.4 km s^{-1} . With these parameters, a radial velocity of $+15.7 \text{ km s}^{-1}$ is predicted for a member at the position of 2RE J0241 – 525. Similarly, Jones (1971) gives a convergent point of $\alpha = 90^\circ.3$, $\delta = -30^\circ.4$ and a group speed of 22.6 km s^{-1} for the Sco–Cen association, which has a spread of ages between 5 and 15 Myr (de Geus, de Zeeuw & Lub 1989). This yields a predicted radial velocity for a kinematic group member at the position of 2RE J0241 – 525 of $+16.9 \text{ km s}^{-1}$. Blaauw (1956) has investigated the Cas–Tau association (see also Walter & Boyd 1991), which has a nuclear age of 20–30 Myr (de Zeeuw & Brand 1985), and gives a convergent point of $\alpha = 86^\circ.0$, $\delta = +4^\circ.9$ and a group speed of 24.1 km s^{-1} . For this association we would predict a radial velocity of $+8.5 \text{ km s}^{-1}$ at the position of 2RE J0241 – 525. The latter three predicted radial velocities are quite close to the observed values for 2RE J0241 – 525, and we could speculate that it is an outlier of one of these loose associations. However, firmer conclusions must await the determination of both a trigonometric parallax and proper motion.

The angular separation of the components of 2RE J0241 – 525 is 22 arcsec. The physical separation depends on orbital inclination and assumed distance, which in turn is dependent on the age of the system. Taking the empirical constraints offered by the Li abundance, an age of 5 to 30 Myr and a distance of between 26 and 50 pc is probable (allowing for the possible 0.3 error in distance modulus). The separation of the components is thus greater than between 570 and 1100 au. If the system has been ejected from a cluster or star formation region, then the gravitational binding energy is equivalent to a change in the system kinetic energy corresponding to a velocity change of less than 1 km s^{-1} . If one were to postulate that the system had been ejected from, say, the IC 2602 or 2391 clusters or the Sco–Cen and Cas–Tau associations, which are at distances of 140–180 pc from 2RE J0241 – 525, then ejection velocities of at least 5 km s^{-1} (for a 30-Myr age) are required. It seems unlikely that the system could emerge intact and with its current binding energy if the system kinetic energy had been increased by more than 20 times that binding energy in a two- or three-body interaction. A similar argument applies to ejection from any nearby cluster, because typical ejection velocities will range between 30 and 200 km s^{-1} (de la Fuente 1995 and private communication). Evaporation from a cluster as a result of many interactions is more feasible, but as escape velocities for clusters like IC 2391 and 2602 are about 1 km s^{-1} , the system could not then reach its present position in its short lifetime. It is much more likely that 2RE J0241 – 525 originated in a gravitationally unbound system, perhaps similar to that now emerging from the Orion nebula, which has an internal dispersion of $3\text{--}4 \text{ km s}^{-1}$ (e.g. Jones & Walker 1988). In that case, 2RE J0241 – 525 could be up to 100 pc from its original birth molecular cloud, which may in any case have dissipated, because Leisawitz, Bash & Thaddeus (1989) have shown that clusters older than about 10 Myr do not have associated molecular clouds.

4 SUMMARY

The optical counterpart to the EUV source 2RE J0241 – 525 has been identified as a pair of chromo-

spherically active, low-mass stars, of spectral types dK7e and dM3e. Both stars are soft X-ray sources and both show signs of rapid rotation. The spatial association of two such active stars, combined with their similar radial velocities lead us to conclude that they form a wide binary system. We have attempted to find the age of the system by isochrone fitting and using the measured Li abundances. The isochrone fitting indicates a pre-main-sequence status, although the age can only be constrained to between 3 and 70 Myr, and the distance to between 19 and 60 pc. An empirical comparison of the $\text{Li I } 6708\text{-\AA}$ EWs with those of similar stars in young clusters and associations lead us to believe that the age of the system is between 5 and 30 Myr, with a corresponding distance of 26 to 50 pc. We stress that caution is required in interpreting the Li abundance, because there is evidence that it does not obey a simple one-to-one relationship with age. The age estimates could be considerably refined if a trigonometric parallax were available, although it is possible that rotation period measurements for the two components may also place further constraints on the system distance.

Although the $\text{H}\alpha$ emission is as strong as one would expect for two such rapidly rotating stars, it is too weak for us to classify 2RE J0241 – 525 as a pair of classical T Tauri stars. Neither is there any infrared detection in the *IRAS* point source catalogue that might indicate that the stars still possess circumstellar material. There is no evidence that the system is linked to any particular star formation region, and only tenuous evidence of a link to any kinematic associations of young stars in the solar vicinity. It seems reasonable therefore to classify 2RE J0241 – 525 as a pair of post-T Tauri stars, rather than weak-lined T Tauri stars which are usually associated with a star formation region. The weak gravitational attraction between the components suggest that they have not been ejected from an open cluster after two- or three-body interactions. It is speculated that the system was born in a gravitationally unbound association and may have drifted by perhaps as much as 100 pc from its original birth site.

ACKNOWLEDGMENTS

We thank the Directors and staff of the Anglo-Australian Observatory, Cerro Tololo Inter-American Observatory, Mount Stromlo Observatory and South African Astronomical Observatory. Their generous allocation of telescope time and assistance has made this paper possible. We also thank Dr David Soderblom for his careful reading of the paper, and Dr Barry Smalley for assistance with the spectral synthesis. RDJ acknowledges the financial support of the UK Particle Physics and Astronomy Research Council (PPARC). Computational work was done on the Birmingham and Keele nodes of the PPARC funded Starlink network.

REFERENCES

- Alexander D. R., Augason G. C., Johnson H. R., 1989, *ApJ*, 345, 1014
- Allan D. J., 1992, *ASTERIX User Note Number 004*, Starlink, Rutherford Appleton Laboratory

- Anders G. J., Jeffries R. D., Kellett B. J., Coates D. W., 1993, *MNRAS*, 265, 941
- Balachandran S., Lambert D. L., Stauffer J. R., 1988, *ApJ*, 333, 267
- Ball B., Bromage G. E., 1995, in Pallavicini R., ed., 9th Cambridge Workshop on Cool Stars, Stellar Systems and the Sun. ASP Conf. Ser., San Francisco, in press
- Barnes T. G., Evans D. S., Moffett T. J., 1978, *MNRAS*, 183, 285
- Basri G., Martín E. L., Bertout C., 1991, *A&A*, 252, 625
- Battinelli P., Capuzzo-Dolcetta R., 1991, *MNRAS*, 249, 76
- Bertout C., 1989, *ARA&A*, 27, 351
- Bessell M., 1979, *PASP*, 91, 589
- Bessell M., 1991, *AJ*, 101, 662
- Blaauw A., 1956, *ApJ*, 123, 408
- Bouvier J., Cabrit S., Fernandez M., Martín E. L., Matthews J. M., 1993a, *A&AS*, 101, 485
- Bouvier J., Cabrit S., Fernandez M., Martín E. L., Matthews J. M., 1993b, *A&A*, 272, 176
- Bowyer S., Lieu R., Lampton S., Lewis J., Wu X., Drake J. J., Malina R. F., 1994, *ApJS*, 93, 569
- Canuto V. M., Mazzitelli I., 1991, *ApJ*, 370, 295
- Collier-Cameron A., Robinson R. D., 1989, *MNRAS*, 236, 57
- Collier-Cameron A., Unruh Y. C., 1994, *MNRAS*, 269, 814
- d'Antona F., Mazzitelli I., 1994, *ApJS*, 90, 467
- David L. P., Harnden F. R. J., Kearns K. R., Zombeck M. V., 1992, *ROSAT Mission Description*, 92-OSSA-16, Appendix F, NRA
- de Geus E. J., de Zeeuw P. T., Lub J., 1989, *A&A*, 216, 44
- de la Fuente R., 1995, *A&A*, 301, 407
- de Zeeuw T., Brand J., 1985, in Boland W., van Woerden H., eds, *Birth and Evolution of Massive Stars and Stellar Groups*. Kluwer, Boston, p. 95
- Doyle J. G., Mathioudakis M., Panagi P. M., Butler C. J., 1990, *A&AS*, 86, 403
- Edwards S. et al., 1993, *AJ*, 106, 372
- Eggen O. J., 1983a, *MNRAS*, 204, 377
- Eggen O. J., 1983b, *MNRAS*, 204, 391
- Eggen O. J., 1991, *AJ*, 102, 2028
- Eggen O. J., 1992, *AJ*, 103, 1302
- Favata F., Barbera M., Micela G., Sciortino S., 1995, *A&A*, 295, 147
- Fekel F. C., 1996, in Strassmeier K. G., ed., *Proc. IAU Symp. 176, Stellar Surface Structure*. Kluwer, Dordrecht, in press
- García-López R. J., Rebolo R., Martín E. L., 1994, *A&A*, 282, 518
- Hale A., 1994, *AJ*, 107, 306
- Herbig G. H., 1978, in Mirzoyan L., ed., *Problems of Physics and Evolution of the Universe*. Academy of Science of Armenia, Yerevan, p. 171
- Innis J. L., Thompson K., Coates D. W., Lloyd Evans T., 1988, *MNRAS*, 235, 1411
- Jeffries R. D., 1993, *MNRAS*, 262, 369
- Jeffries R. D., 1995, *MNRAS*, 273, 559 (J95)
- Jeffries R. D., Byrne P. B., Doyle J. G., Anders G. J., James D. J., Lanzafame A. C., 1994a, *MNRAS*, 270, 153
- Jeffries R. D., James D. J., Bromage G. E., 1994b, *MNRAS*, 271, 476
- Jeffries R. D., Bertram D., Spurgeon B. R., 1995, *MNRAS*, 276, 397
- Jonson H., 1966, *ARA&A*, 4, 193
- Jones B. F., Walker M. F., 1988, *AJ*, 95, 1755
- Jones D. H. P., 1971, *MNRAS*, 152, 231
- Kirkpatrick D., Kelly D., Rieke G., Liebert J., Allard F., Wehrse R., 1993, *ApJ*, 402, 643
- Kurucz R. L., 1991, in Davis Philip A. G., Uggren A. R., Janes K. A., eds, *Precision Photometry: Astrophysics of the Galaxy*. L. Davis Press, Schenectady, p. 27
- Kurucz R. L., Bell B., 1995, Technical Report, Smithsonian Astrophysical Observatory
- Lada C. J., Lada E. A., 1991, in Janes K., ed., *The Formation and Evolution of Star Clusters*. Astron. Soc. Pac., San Francisco, p. 3
- Leisawitz D., Bash F. N., Thaddeus P., 1989, *ApJS*, 70, 731
- Lyngå G., 1987, Technical Report, Lund Observatory
- Magazzù A., Rebolo R., Pavlenko Y. V., 1992, *ApJ*, 392, 159
- Martín E. L., Brandner W., 1995, *A&A*, 294, 744
- Martín E. L., Magazzù A., Rebolo R., 1992, *A&A*, 257, 186
- Martín E. L., Rebolo R., Magazzù A., Pavlenko Y. V., 1994, *A&A*, 282, 503
- Mason K. O. et al., 1995, *MNRAS*, 274, 1194
- Mathioudakis M., 1992, PhD thesis, Queens Univ., Belfast
- Menzies J. W., Cousins A. W. J., Banfield R. M., Laing J. D., 1989, *SAAO Circ.*, 13, 1
- Mills D., Webb J., 1994, Starlink User Note 152.1, Rutherford Appleton Laboratory
- Neuhäuser R., Sterzik M. F., Schmitt J. H. M. M., Wichmann R., Krautter J., 1995a, *A&A*, 297, 391
- Neuhäuser R., Sterzik M. F., Torres G., Martín E. L., 1995b, *A&A*, 299, L13
- Pallavicini R., Pasquini L., Randich S., 1992, *A&A*, 261, 245
- Pavlenko Y. V., Rebolo R., Martín E. L., García-López R. J., 1995, *A&A*, 303, 807
- Pfeffermann E. et al., 1986, *Proc. SPIE*, 733, 519
- Pounds K. A. et al., 1993, *MNRAS*, 260, 77
- Prosser C. F., Stauffer J. R., Kraft R. P., 1991, *AJ*, 101, 1361
- Pye J. P., Hodgkin S. T., Stern R. A., Stauffer J. R., 1994, *MNRAS*, 266, 798
- Pye J. P. et al., 1995, *MNRAS*, 274, 1165
- Randich S., Schmitt J. H. M. M., Prosser C. F., Stauffer J. R., 1995, *A&A*, 300, 134
- Robinson R. D., Carpenter K. G., Slee O. B., Nelson G. J., Stewart R. T., 1994, *MNRAS*, 267, 918
- Schmidt-Kaler T., 1982, in Schaifers K., Vogt H. H., eds, *Physical Parameters of the Stars*, Landolt-Bornstein New Series, Vol. 2b. Springer-Verlag, New York
- Smith K. C., 1992, PhD thesis, Univ. London
- Soderblom D. R., Jones B. F., Balachandran S., Stauffer J. R., Duncan D. K., Fedele S. B., Hudon J. D., 1993a, *AJ*, 106, 1059
- Soderblom D. R., Stauffer J. R., Hudon J. D., Jones B. F., 1993b, *ApJS*, 85, 315
- Soderblom D. R., Henry T. J., Shetrone M. D., Jones B. F., Saar S. H., 1996, *ApJ*, 460, in press
- Spencer-Jones J. H., 1980, *Mon. Notes Astron. Soc. S. Afr.*, 39, 89
- Stauffer J. R., 1991, in Catalano S., Stauffer J. R., eds, *NATO ASI Series: Angular Momentum Evolution of Young Stars*. Kluwer, Dordrecht, p. 117
- Stauffer J. R., Hartmann L. W., 1986, *ApJS*, 61, 531
- Stauffer J. R., Hartmann L. W., Jones B. F., McNamara B. R., 1989a, *ApJ*, 342, 285
- Stauffer J. R., Hartmann L. W., Jones B. F., 1989b, *ApJ*, 346, 160
- Stauffer J. R., Giampapa M. S., Herbst W., Vincent J. M., Hartmann L. W., Stern R. A., 1991, *ApJ*, 374, 142
- Stauffer J. R., Caillault J. P., Gagné M., Prosser C. F., Hartmann L. W., 1994a, *ApJS*, 91, 625
- Stauffer J. R., Liebert J., Giampapa M. S., Macintosh B., Reid N., Hamilton D., 1994b, *AJ*, 108, 160
- Stauffer J. R., Hartmann L. W., Barrado y Navascues D., 1995, *ApJ*, 454, 910
- Sterzik M. F., Alcalá J. M., Neuhäuser R., Schmitt J. H. M. M., 1995, *A&A*, 297, 418
- Stone R. P. S., Baldwin J. A., 1983, *MNRAS*, 204, 347

Swenson F. J., Stringfellow G. S., Faulkner J., 1990, ApJ, 348, L33
Tagliaferri G., Cutispoto G., Pallavicini R., Randich S., Pasquini L., 1994, A&A, 285, 272
Tonry J. L., Davis M., 1979, AJ, 84, 1511

Walter F. M., Boyd W. T., 1991, ApJ, 370, 318
Walter F. M., Brown A., Mathieu R. D., Myers P. C., Vrba F., 1988, AJ, 96, 297
Young A., Skumanich A., Harlan E., 1984, ApJ, 282, 683